CHEMISTRY
A EUROPEAN JOURNAL

DOI: 10.1002/chem.201000339

Luminescent Ionic Liquid Crystals from Self-Assembled BODIPY Disulfonate and Imidazolium Frameworks**

Jean-Hubert Olivier,[a] Franck Camerel,[a] Gilles Ulrich,[a] Joaquín Barberá,*[b] and Raymond Ziessel*[a]

Abstract: A series of modular mesogenic salts based on the combination of anionic 4,4-difluoro-4-bora-3a,4a-diaza-*s*-indacene (*F*-BODIPY) 2,6-disulfonate dyes and trialkoxybenzyl-functionalised imidazolium cations has been designed and synthesised. Each salt contains a rigid dianionic BODIPY core associated with two imidazolium cations functionalised by 1,2,3-trialkoxybenzyl (alkyl = *n*-C_8, *n*-C_{12} or *n*-C_{16}) units or, in one case, with imidazolium cations functionalised by a trialkylgallate (3,4,5-trialkoxybenzoate) unit in which the 3,5-dialkyl groups are terminated with a polymerisable acrylate entity. All these compounds were highly fluorescent in solution with quantum yields ranging from 54 to 62%. In the solid state, the width of the emission band observed at around 650 nm is a clear signature of aggregation. With the trialkoxybenzylimidazolium cations, polarised optical microscopy (POM) and X-ray scattering experiments showed that columnar mesophases were formed. Differential scanning calorimetry (DSC) studies confirmed the mesomorphic behaviour from room temperature to about 130°C for salts with alkyl chains containing 8, 12 and 16 carbon atoms. The strong luminescence of the BODIPY unit was maintained in the mesophase and fluorescence measurements confirmed the presence of *J* aggregates in all cases. The salt containing the gallate-functionalised imidazolium cations showed no mesomorphism but the acrylate terminal units could be used to engender photoinitiated polymerisation thereby allowing the material to be immobilised on glass plates. The polymerisation process was followed by FTIR spectroscopy and the fixed and patterned films were highly fluorescent with a solid-state emission close to that of the complex in the solid state.

Keywords: aggregation · fluorescence · liquid crystals · polymerization · self-assembly

Introduction

Over the past decade a myriad of fascinating liquid crystals (LC) have been engineered,[1] some of them designed for charge separation and thus finding application, for example, in solar cells.[2] A recent development has been the combination of amphiphilic cations and anions to give salts termed ionic liquid crystals (ILCs), their synthesis being referred to as "ionic self-assembly" (ISA). These soft materials combine the properties of ionic liquids (ILs) and LCs and they have already found application in ionic conductors,[3] batteries[4] and energy-conversion devices.[5] In most instances the mesogenic properties derive from the amphiphilicity of the cationic component, typically an ammonium,[6,7] imidazolium[8] or piperidinium[9] derivatives. The counteranion is considered to be present essentially for charge compensation, although it does affect the mesophase stability and the clearing temperature.[10] Nonetheless, examples are known in which modification of the anion produces ILCs with interesting new properties. For example, anions that contain π-conjugated chromophores can be incorporated to yield luminescent ionic liquid crystals.[11]

If functional groups such as acrylate entities are incorporated into ILCs, the possibility arises of polymerisation after mesophase formation to generate ordered ionic polymer films. Columnar mesophases of an acrylate-functionalised

[a] J.-H. Olivier, Dr. F. Camerel, Dr. G. Ulrich, Dr. R. Ziessel
LCOSA, ECPM, Université de Strasbourg-CNRS
25 rue Becquerel, 67008 Strasbourg Cedex (France)
Fax: (+33) 368-85-27-61
E-mail: ziessel@unistra.fr

[b] Dr. J. Barberá
Departamento de Química Orgánica
Instituto de Ciencia Materiales de Arágon
Universidad de Zaragoza-CSIC, 50009 Zaragoza (Spain)
Fax: (+34) 976-761209
E-mail: jbarbera@unizar.es

[**] BODIPY = 4-bora-3a,4a-diaza-*s*-indacene.

Supporting information for this article is available on the WWW under http://dx.doi.org/10.1002/chem.201000339.

ILC have indeed been shown to be polymerisable under UV irradiation, this reaction freezing the columnar organisation and producing enhanced ionic conductivity in comparison with the monomer mesophase.[12]

Among π-conjugated chromophores, 4,4-difluoro-4-bora-3a,4a-diaza-*s*-indacene (*F*-BODIPY) dyes have become very popular as a result of their special optical properties.[13] These include high photostability, high absorption coefficients (ranging from 80000 to about 200000 $M^{-1}cm^{-1}$) in the visible portion of the electromagnetic spectrum, narrow emission profiles and exceptional emission quantum yields that reach 100% in the best cases. Of particular use are the variety and facility of chemical modifications possible at the dipyrromethene core, at the central pseudo-*meso* position and also at the boron atom.[14] In general this is not true for other common fluorophores and the ability to prepare water-soluble BODIPY derivatives is particularly advantageous in ISA. BODIPY dyes have already found applications in solar cells,[15] as molecular probes,[16] as pH sensors[17] and in OLED devices.[18] Their incorporation into LCs should facilitate control of the anisotropy of their intermolecular ordering, a crucial influence on the electronic performance of such devices. Previous work has in fact shown that mesomorphic π-conjugated dyes are not readily accessible and that their syntheses are often complex involving multistep processes.[19]

An elegant solution to the problem of the efficient synthesis of fluorescent ILCs is the application of ISA based upon the supramolecular association of a central multicharged organic core with amphiphilic counterions.[20] When the balance between the charges, the rigid core and the flexible chains (of the counterions) is optimal, hierarchical superstructures can be generated through electrostatic interactions between charged amphiphiles and oppositely charged oligoelectrolytes as the primary interaction aided by hydrophobic and π–π interactions as secondary driving forces to promote self-organisation. Additional interactions, such as hydrogen-bonding, can also be introduced to further stabilise and control the organisation of the assemblies.[21,22] This process of construction of liquid-crystalline materials based on multiple non-covalent interactions allows for an easy tuning of the properties of the emergent structures by careful choice of the alkyl volume fraction (internal solvent) through simple exchange of the binding partner in the corresponding assembly step without tedious synthetic operations.

Herein we describe the formation of columnar ionic liquid-crystalline materials from a fluorescent dianionic BODIPY derivative and amphiphilic imidazolium countercations by an ISA process. Imidazolium cations carrying trialkoxybenzyl moieties (alkoxy = *n*-C_8H_{17}, *n*-$C_{12}H_{25}$ or *n*-$C_{16}H_{33}$) were chosen for the induction of the mesogenic properties and the BODIPY disulfonate ($BODDS^{2-}$) dianion to provide the fluorophore. The optical properties were studied in solution and in the solid state to evaluate the presence of aggregates. In addition, luminescent ionic polymeric films were engendered by photopolymerisation of the salt produced by using an imidazolium cation functionalised with trialkylgallate units in which two of the alkyl groups have terminal acrylate units.

Results and Discussion

The ion association complexes (salts) formed between the BODIPY disulfonate ($BODDS^{2-}$) dianion and various imidazolium cations are shown in Scheme 1. 1-Methyl-3-(3,4,5-trialkoxybenzyl)imidazolium chlorides, [$C_n$benzyl]Cl, were synthesised as previously described by reaction of 1-methylimidazole and the corresponding 3,4,5-trialkoxybenzyl chlorides (n = 8, 12, 16) in toluene at 80 °C overnight.[3b,23] The imidazolium derivative carrying two polymerisable acrylate units, P_{12}gall, with chloride as the counterion was synthesised as described in the literature.[24] 2,6-Disulfonato-1,3,5,7,8-pentamethyl-4,4-difluoro-4-bora-3a,4a-diaza-*s*-indacene (Na_2BODDS) with sodium as the counterion was also prepared according to a published procedure.[25] The complexes were obtained by dissolution of the reactants in hot DMF followed by precipitation with water. BODDS-C_{12}benzyl and BODDS-C_{16}benzyl were recrystallised from hot DMSO, BODDS-C_8benzyl was recrystallised from a CH_2Cl_2/AcOEt solution by slow evaporation of the dichloromethane and BODDS-P_{12}gall was purified by recrystallisation from hot cyclohexane. Complexation in a 2:1 ratio was unambiguously confirmed by elemental analysis and NMR spectroscopy. In particular, the proton signals at $\delta = 7.79$ and 7.67 ppm, characteristic of the imidazolium fragment, had twice the intensity of the BODDS methyl signals at $\delta = 2.66$, 2.62 and 2.59 ppm. The ^{1}H NMR spectrum of the BODDS-C_{12}benzyl complex is given in Figure 1 as a representative example. Some trials were performed with an imidazolium derivative carrying three acrylic polymerisable functions but isolation of a stoichiometric ion associate was unsuccessful.

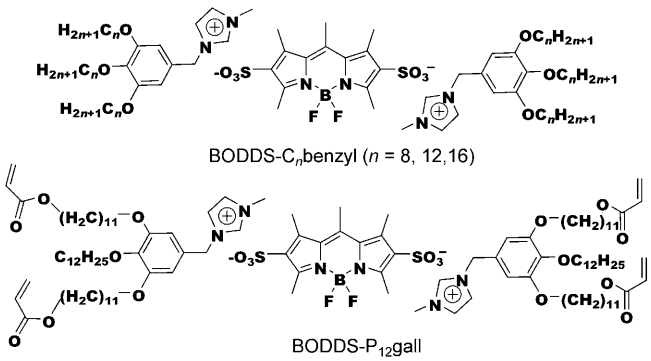

Scheme 1. Structures of BODDS-$C_n$benzyl (n = 8, 12, 16) and BODDS-P_{12}gall.

All the complexes are strongly luminescent in solution and in the solid state. In dichloromethane solution, all the BODIPY complexes show an intense $S_0 \rightarrow S_1$ transition at around 507 nm with an extinction coefficient of around

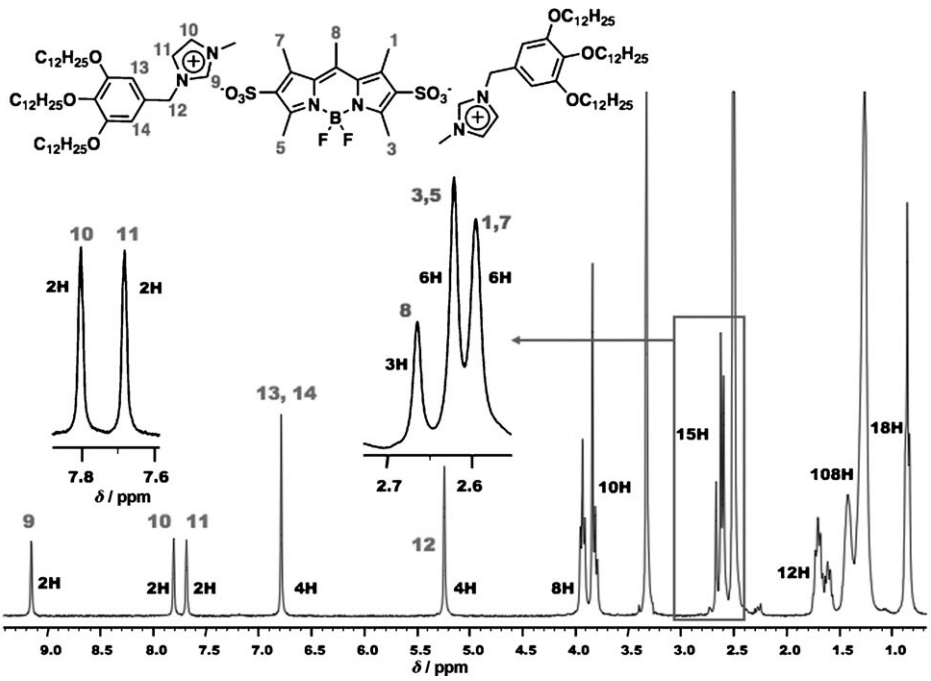

Figure 1. ^{1}H NMR spectrum of the BODDS-C_{12}benzyl complex in [D_6]DMSO at room temperature, including peak assignments and integrals.

70000–85000 $M^{-1}cm^{-1}$, assigned to π–π* transitions of the boradiazaindacene chromophore (Table 1). A weak and broad band located at 365 nm has been attributed, in the light of previous results, to the $S_0 \rightarrow S_2$ (π–π*) transition of the boradiazaindacene core.[26] Excitation at 490 nm ($S_0 \rightarrow S_1$ transition) leads to a strong emission at 532 nm with quantum yields in the range of 50–65%, typical of BODIPY dyes (Figure 2). The fluorescence band shows good mirror symmetry with the lowest-energy absorption band and the quantum yield is not sensitive to the presence of oxygen. Both characteristics are in keeping with the radiative relaxation of a singlet excited state. Note that the optical properties are not affected by the nature of the counterion in dilute solution. No evidence was found for the formation of columnar aggregates in solution as previously observed for perylene bisimide derivatives.[27]

Table 1. Spectroscopic data for the BODDS-$C_n$benzyl (n=8, 12, 16) and BODDS-P_{12}gall salts.

Compounds	λ_{abs}[a] [nm]	ε[a] [$M^{-1}cm^{-1}$]	λ_F[a] [nm]	Φ_F[b]
BODDS-C_8benzyl	507	78400	532	0.54
BODDS-C_{12}benzyl	507	85300	532	0.62
BODDS-C_{16}benzyl	507	71400	532	0.57
BODDS-P_{12}gall	507	86400	532	0.58

[a] Measured in CH_2Cl_2, at room temp. [b] Determined in dichloromethane solution with a salt concentration of ca. 5×10^{-7} M and by using Rhodamine 6G as a reference (Φ=0.78 in water, λ_{exc}=488; see ref. [28]. All Φ_F values are corrected for changes in the refractive index.

Solid-state fluorescence spectra were recorded at room temperature by using a spectrofluorimeter equipped with an optical fibre probe. The luminescence spectrum of the solid BODDS-C_{12}benzyl complex displays a broad emission band centred at 677 nm (Figure 3). This emission, which is strongly redshifted ($\Delta\lambda\approx145$ nm) relative to that in solution, is attributed to aggregated species.[29] The emission spectrum of the BODDS-P_{12}gall complex extends from 500 to 750 nm with two distinct maxima at 603 and 666 nm. The shoulder at 557 nm is attributed, on the basis of the measurements in solution, to the emission of the monomeric species and the redshifted bands are due to the emission

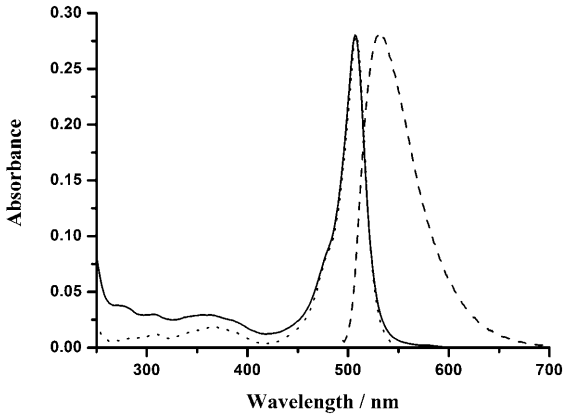

Figure 2. Absorption (solid line) and excitation (dotted line) spectra for BODDS-C_{16}benzyl and its emission spectrum (dashed line; λ_{exc}= 490 nm). All spectra were measured in CH_2Cl_2 at room temperature (c= 4×10^{-6} M).

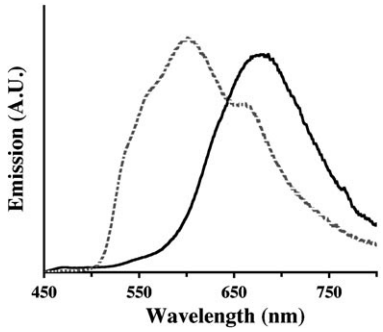

Figure 3. Solid state emission spectra of BODDS-C_{12}benzyl (solid line) and BODDS-P_{12}gall (dashed line) measured at room temperature (λ_{ex}= 390 nm).

of aggregated BODIPY species. The emission band at 602 nm is likely due to dimeric species (excimers) and the one at 666 nm to larger aggregates.[19a] These solid-state emission studies seem to indicate that the microsegregation, that is, the confinement of the BODIPY fragments, is probably less effective with $P_{12}gall^+$ cations as a consequence of the structural and polarity changes imported by the ester groups. This will have a massive effect on the thermal behaviour of the compound (see below).

The thermotropic properties of BODDS-$C_n$benzyl ($n=8$, 12, 16) and BODDS-P_{12}gall were investigated by a combination of differential scanning calorimetry (DSC), polarising optical microscopy (POM) and small-angle X-ray diffraction studies (XRD). DSC measurements, POM analysis and NMR spectroscopy revealed that the complexes are stable up to 180 °C. DSC traces of BODDS-C_8benzyl and BODDS-C_{12}benzyl display a reversible transition centred at 126 and 128 °C, respectively (see the Supporting Information). POM observations showed that these compounds are in an isotropic state above these temperatures. On cooling from the isotropic melt, pseudo-fan-shaped textures, characteristic of columnar mesophases, rapidly developed (Figure 4). For the compound BODDS-C_8benzyl, a glass transition can also be observed at around 20–30 °C (more marked on the endotherms). Well-defined POM observations showed that below T_g the material is a brittle and birefringent solid and that above T_g the compound is a soft, viscous and malleable material but still birefringent. The observed glass transition may indicate a slow crystallisation of the material at low temperature. These results suggest that BODDS-C_8benzyl and -C_{12}benzyl are in a liquid-crystalline state from the glass transition observed at around room temperature up to the true liquefaction temperature at around 125 °C. The BODDS-C_{16}benzyl compound displays a single reversible transition centred at 40 °C in the explored temperature range of 0–180 °C. POM observations showed that this compound is birefringent and in a gel state above this transition. The observation of birefringence in the fluid state at high temperatures confirmed its liquid-crystalline nature. The observed transition, which is associated with a large enthalpy change ($\approx 68\ kJ\ mol^{-1}$), is attributed to a crystal-to-mesophase transformation. The initial DSC heating curve of the BODDS-P_{12}gall complex display a broad endotherm centred at 47 °C and POM observations confirmed that the compound melts to an isotropic state above this transition. On cooling, the material remained in an isotropic state down to −30 °C and no other transitions were detected by DSC in the temperature range −30 to 180 °C. It appears that this compound has no mesomorphic properties and that the thermodynamically stable liquid state of this material is isotropic and disordered.

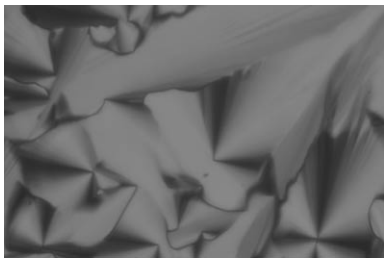

Figure 4. BODDS-C_{12}benzyl viewed by optical microscopy under crossed-polarisers (symbolised by the cross in the corner of the picture) at 100 °C on cooling. The texture exhibits birefringent pseudo-fan shapes indicative of a columnar phase.

To confirm the previous POM and DSC observations, wide- (WAXS) and small-angle (SAXS) X-ray scattering measurements at different temperatures were undertaken. The experiments were performed in the following order: 1) room temperature in the virgin state, 2) room temperature after heating to the isotropic liquid and 3) at high temperature. The room-temperature experiments were performed before the high-temperature experiments in case any of the compounds were thermally unstable. The results are presented in Table 2.

Table 2. X-ray measurements on the liquid-crystalline phases of BODDS-$C_n$benzyl ($n=8$, 12, 16).[a]

Compound	Transition temperatures [°C] (ΔH [kJ mol^{-1}])	Mesophase	d_{meas} [Å]	I	hk	d_{calcd} [Å]	Mesophase parameters measured at T	M [g mol^{-1}]
BODDS-C_8benzyl	Cr 25 Col_h 128 (1.54) Iso	Col_h	31.2	VS	10	31.4	$T=110$ °C	1536
	Iso 124.5 (−1.46) Col_h		15.9	M	20	15.7	$a=36.3$ Å	
			4.4	br			$S=1140$ Å^2	
BODDS-C_{12}benzyl	Col_h 129.5 (0.67) Iso	Col_h	38.9	VS	10	39.0	$T=25$ °C[b]	1873
	Iso 126 (−0.67) Col_h		22.7	M	11	22.5	$a=45.0$ Å	
			19.4	M	20	19.5	$S=1755$ Å^2	
			4.4	br				
			35.7	VS	10	35.5	$T=114$ °C	
			17.7	M	20	17.8	$a=41.0$ Å	
			4.4	br			$S=1455.5$ Å^2	
BODDS-C_{16}benzyl	Cr 47.5 (67.20) Col_h	Col_h	39.1	VS	10	39.1	$T=120$ °C	2208
	Col_h 33.6 (−69.88) Cr		4.6	br			$a=45.1$ Å	
							$S=1763$ Å^2	

[a] Cr: crystalline phase; Iso: Isotropic liquid; Col_h: hexagonal columnar mesophase. d_{meas} and d_{calcd} are the measured and calculated diffraction spacing, I is the intensity of the reflection (VS: very strong; S: strong; M: medium; W: weak; br: broad), h and k are the indexations of the reflections corresponding to the two-dimensional hexagonal lattice of the Col_h phase, a is the lattice parameter of the hexagonal columnar phase ($a=\frac{2}{\sqrt{3}}\times<d_{10}>$ in which $<d_{10}>=\frac{1}{N_{hk}}\left(\sum_{h,k} d_{hk}\sqrt{h^2+k^2+hk}\right)$ and N_{hk} is the number of hk reflections) and S is the hexagonal lattice area ($S=a\times<d_{10}>$ for Col_h). [b] After thermal treatment.

All the compounds showed 3D crystalline phases in their virgin state. BODDS-C_8benzyl and -C_{16}benzyl recrystallised after thermal treatment, whereas BODDS-C_{12}benzyl remained in the liquid-crystal state at room temperature. These observations are in line with the previous DSC and POM observations. The three complexes provided X-ray patterns characteristic of a liquid-crystal phase at high temperatures (see Table 2). This was deduced from the presence of one or two sharp reflections in the low-angle region and the absence of scattering in the high-angle region except for a broad diffuse halo characteristic of the liquid-like order of the hydrocarbon chains. The set of one or two reflections found in the low-angle region at high temperatures has two possible interpretations. 1) The diffraction peak(s) can be the first (and second)-order reflection(s) from a layer structure (smectic mesophase). In this case the spacing of the first reflection (or the double of the second reflection) is the layer thickness *d*. 2) The peak(s) is (are) the 100 (and 200) reflection(s) from a hexagonal columnar mesophase, the (110) reflection being absent.

The second interpretation is the more reasonable for the following reasons. 1) The hexagonal symmetry of the mesophase of BODDS-C_{12}benzyl was unambiguously established at room temperature (Table 2 and Figure 5). 2) The observed textures are characteristic of columnar mesophases (see Figure 4). 3) The $C_n$benzyl$^+$ cations contain three long chains attached to the aromatic unit and the spatial requirements of these chains are impossible to fulfil in a smectic structure owing to the mismatch between the cross-section of the aromatic moiety and the total cross-section of the hydrocarbon chains.[30] Instead, the chains have more space available in a columnar structure in which they spread out around the central core of the column. 4) If the mesophase is smectic, very simple calculations allow the molecular cross-section to be the estimated as follows: if the density is known, the molecular volume can be deduced from the molecular mass according to $V_m = M/(0.6022\rho)$ in which V_m is the molecular volume in Å^3, M is the molecular mass and ρ is the density in g cm^{-3}. Then, dividing the molecular volume by the layer thickness (d) gives the cross-section of a molecule in the plane of the smectic layer. The hypothetical molecular cross-section at high temperatures would be $80/\rho$, $88/\rho$ and $94/\rho$ Å^2 for BODDS-C_8benzyl, -C_{12}benzyl and -C_{16}benzyl, respectively. Because the density must be similar for the three compounds (in fact, it is usually assumed that density is close to 1 g cm^{-3} for organic compounds), this would mean that the cross-section increases upon increasing the number of carbon atoms in the chains (18% from $n=8$ to $n=16$). This is not consistent with a smectic structure because lengthening the hydrocarbon chains should increase the length of the molecule but not its width. On the other hand, if the mesophase is columnar hexagonal and we deduce the molecular volume V_m by using the above-mentioned equation then the height of column h occupied by each molecule can be estimated as $h = V_m/S$, with S the area of the two-dimensional hexagonal cell ($S = a < d_{10} >$). The results of these calculations for high temperatures are $h = 2.22/\rho$, $2.14/\rho$ and $2.14/\rho$ Å for BODDS-C_8benzyl, -C_{12}benzyl and -C_{16}benzyl, respectively. The variation is only 6%, that is, the estimated values for h are practically the same for the three compounds. This is consistent with the mesophase being columnar because, for this kind of mesophase, lengthening the hydrocarbon chains is expected to increase only the diameter of the column but not the stacking distance. It is clear that a single molecule cannot be located in a "slice" of about 2.1–2.2 Å thickness, but it is reasonable that two molecules are contained in a "slice" of 4.2–4.4 Å, assuming a density of 1 g cm^{-3} (4.7–4.9 Å if the density is 0.9 g cm^{-3}). The S values for the three compounds at high temperatures are, respectively, 1140, 1455.5 and 1763 Å^2. These values follow a logical evolution as they are proportional to the molecular masses. Furthermore, the smaller hexagonal lattice constant found for BODDS-C_{12}benzyl at 114 °C relative to that at room temperature (see Table 2) is consistent with the higher conformational freedom of the hydrocarbon chains. In agreement with this, the estimated h value at room temperature is $1.77/\rho$ Å, a smaller value than that found at 114 °C, and the estimated S value is 1755 Å^2, a larger value than that found at 114 °C.

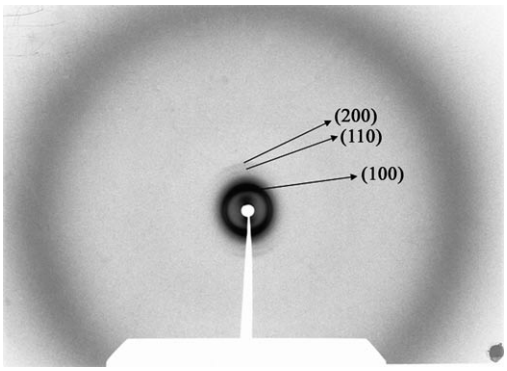

Figure 5. XRD patterns of the BODDS-C_{12}benzyl complex in the hexagonal columnar phase at room temperature after thermal treatment.

The previous calculations imply that each "disc" generating the columns through stacking contains two complexes. A structural model can be depicted as follows: the head groups of the cations contact the central pairs of coplanar dianions thus causing the peripheral chains to surround the central ionic region. In this way, an optimal micro-segregation between the aliphatic and polar parts is assured. The hydrocarbon chains are able to efficiently fill the peripheral space around the columnar core and the mutual organisation of the columns into a hexagonal lattice leads to the formation of the mesophase (Figure 6). However, the proposed arrangement for the molecular stacking within the columns is probably an oversimplified model because, in fact, aggregation may take place in such a way that the molecules contained in a "slice" are not in the same plane with just their tips pointing towards the column core without the need to form discrete discs. Thus, the columns have an aromatic continuum in the core and an aliphatic continuum in the periph-

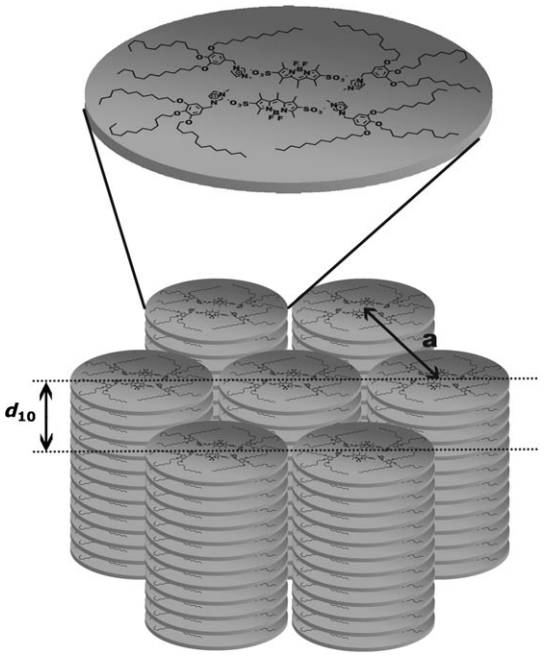

Figure 6. Proposed model of BODDS-C_{12}benzyl in a hexagonal columnar mesophase ($d_{10}=3.9$ nm, $a=4.5$ nm).

ery. Geometrical calculations performed on the hexagonal mesophases by Kato and co-workers with imidazolium derivatives and BF_4^- as the anion revealed that the plateau also has a thickness of 4.4 Å and contains four C_{12}benzyl$^+$ or P_{12}gall$^+$ cations.[3a,23] It seems that the mesophase geometry is imposed by the shape of the imidazolium fragments and the plateau are always formed by four cations associated to four monoanions or two dianions. Only the parameter *a* is affected by the nature, size and number of anions (monoanion or dianion). The lateral extension of the column varies as a function of the size and number of anions, but the thickness and the number of imidazolium fragment forming the plateau remain constant.

Compound BODDS-C_{12}benzyl is highly luminescent in the liquid-crystalline state upon excitation at 380 nm (Figure 7). The observed red luminescence confirmed the measurements obtained by fluorescence spectroscopy on the

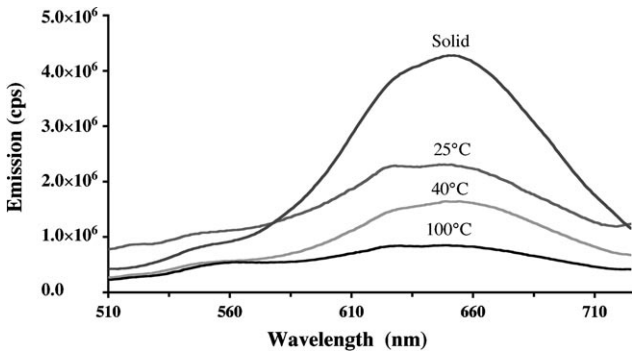

Figure 7. Emission spectra of BODDS-C_{12}benzyl measured in the mesophase at different temperatures ($\lambda_{ex}=380$ nm).

powdered solid (Figure 3) and indicate the same kind of aggregated species to be present in the mesophase. Similar fluorescence peaks were observed at around 540, 621 and 650 nm, their relative intensities being slightly temperature-dependent. The luminescence intensity decreased on increasing the temperature and this process appeared to be reversible, excepting the degradation of the samples, as confirmed by NMR spectroscopy at the end of the thermal studies.

XRD experiments performed on the BODDS-P_{12}gall complex at 150 °C and at room temperature after thermal treatment showed that this compound is amorphous and non-mesogenic. Nevertheless, it was found to be able to form good quality films after evaporation of dichloromethane solutions on flat glass surfaces. Taking advantage of the presence of the acrylate groups, photopolymerisation experiments were performed to immobilise the fluorescent $BODDS^{2-}$ anions in a fixed polymeric matrix. For this purpose, BODDS-P_{12}gall solutions in dichloromethane at $c=10^{-3}$ mol L^{-1} containing 10 % w/w of 1-hydroxycyclohexyl phenyl ketone as photoinitiator were deposited on clean glass cover-slides and the solvent was left to slowly evaporate in air. After drying and thermal treatment at 65 °C, the coloured films were exposed to UV irradiation ($\lambda=365$ nm, 5 mW cm^{-2}) for 60 min at 30 °C. Note that the BODIPY fragments were not expected to prevent the photopolymerisation due to their low absorption at 365 nm (see above). The effectiveness of the polymerisation was established by the insolubility of the films in dichloromethane after exposure. The extent of acrylate polymerisation was determined to be around 85 % by using FTIR spectroscopy to monitor the disappearance of the acrylate band at 810 cm^{-1}. The effect on the other acrylate band at 1637 cm^{-1} is masked by the presence of the ester function present between the imidazolium and the gallate fragments. However, it is clear that not all the acrylate groups react under the applied conditions.

POM showed that the material remained in an isotropic state after the photopolymerisation experiments and no thermal transitions were detected by DSC in the temperature range of 0–200 °C. Interestingly, masks can be used during the photopolymerisation experiments to limit the irradiation to a specific area. In this way it was possible to pattern luminescent molecules into a fixed polymer matrix (Figure 8a). The unexposed parts were easily removed by flowing dichloromethane over the films. Under UV light, the polymeric films were strongly luminescent (Figure 8b). Solid-state emission measurements gave results similar to those measured for the solid BODDS-P_{12}gall. The emission spectrum of the polymerised films measured at room temperature take the form of a broad band extending from 500 to 800 nm with two distinct maxima at 540 and 620 nm testifying to the presence of monomeric and larger BODIPY aggregates (Figure S4). The relative intensities of the bands indicate that the polymerisation isolated or created more aggregated species inside the films (see the Supporting Information). The evolution of the distribution of the various

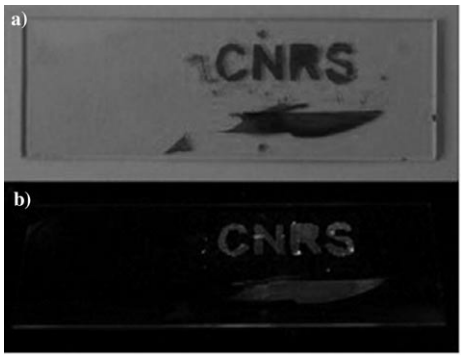

Figure 8. a) Polymerised film of BODDS-P_{12}gall observed under white light. b) Same patterned film observed under UV light. (CNRS represents the Centre National de La Recherche Scientifique (host research institution)).

species inside the film can also be affected by the preparation and thermal history of the sample. These results demonstrate that it is possible to prepare luminescent polymeric materials by the photopolymerisation of self-assembled luminescent and polymerisable ion associates. Attempts to remove the ionically bound dye failed under the following conditions: 1) aqueous 1 M NaCl solutions to saturated (brine) and 2) an aqueous concentrated NaCl/dimethylformamide mixture at 80 °C during one night. Under all attempted conditions only trace amounts of the fluorophore were detected by UV/Vis absorption spectroscopy, which proves that the alkyl matrix is very robust and further modification will be difficult.

Conclusion

A series of functional salts have been synthesised by ionic self-assembly from a charged fluorescent BODIPY disulfonate core and various types of non-luminescent amphiphilic imidazolium monocations. Acrylate units as terminal groups on the cation substituents proved useful for the polymerisation of deposited films of the salt. A stoichiometry of 1:2 (dye to imidazolium) for all the salts was established by ^{1}H NMR spectroscopy and elemental analysis. Solid-state fluorescence measurements performed on the pristine BODDS-C_{12}benzyl solid showed the emission to be strongly redshifted and broadened (spanning over 200 nm) compared with the narrow fluorescence (about 50 nm) in dilute solution. Multiple peaks in the fluorescence spectrum are considered to indicate the presence of aggregated species. Interestingly, for the BODDS-P_{12}gall solid the redshift is less pronounced with major transitions localised at 603 and 666 nm. This complex is slightly less prone to aggregation compared with the genuine benzyl-grafted derivatives BODDS-$C_n$benzyl. The use of imidazolium cations with trialkoxybenzyl substituents enables the formation of columnar mesophases with hexagonal symmetry, unambiguously identified by X-ray scattering measurements and by the typical textures observed between crossed-polarisers by optical microscopy. From these data it is estimated that for the BODDS-$C_n$benzyl complexes, pairs of BODIPY dianions associated with four imidazolium cations form discs able to stack in a column. Solid-state fluorescence measurements in the columnar mesophases showed that the BODIPY dianions were not isolated and that *J* aggregates formed inside the mesophases, a result in keeping with the solid-state measurements. The BODDS-P_{12}gall complex shows no mesomorphic behaviour but is easily polymerisable under mild conditions in the presence of a radical photoinitiator allowing information to be written on the fixed polymeric film. Within the films, the dye remains strongly fluorescent with a wavelength of emission bathochromically shifted compared with that in solution, which confirms the formation of aggregates in the polymer. Worth noting is the high chemical and photochemical stability of the BODIPY dyes even in the presence of reactive radicals generated during the photopolymerisation process. The use of ionic self-assembled complexes provides a facile tool to produce liquid-crystalline materials and thin films stable over a large temperature range. Application to optical memories in which writing, reading and erasing cycles are required is currently in progress.

Experimental Section

General methods: The 300 (^{1}H), 400 (^{1}H) and 75.5 MHz (^{13}C) NMR spectra were recorded at room temperature by using perdeuterated solvents as internal standards. A ZAB-HF-VB-analytical apparatus in FAB+ mode was used with *m*-nitrobenzyl alcohol (*m*-NBA) as matrix. Chromatographic purification was conducted by using 40–63 μm silica gel. Thin layer chromatography (TLC) was performed on silica gel plates coated with fluorescent indicator. FT-IR spectra were recorded by using a Perkin-Elmer "spectrum one" spectrometer equipped with an ATR diamond apparatus. UV/Vis spectra were recorded by using a Shimadzu UV-3600 dual-beam grating spectrophotometer with a 1 cm quartz cell. Fluorescence spectra were recorded on a HORIBA Jobin–Yvon fluoromax 4P spectrofluorimeter with a 1 cm quartz cell for solutions or an optical fiber for solids. Temperature-dependent luminescence measurements were performed on thin films thank to the HORIBA Jobin-Yvon fluoromax 4P spectrofluorimeter equipped with an optical fiber and a heating stage (Linkam LTS350 hot-stage and a Linkam TMS94 central processor). All fluorescence spectra were corrected. The fluorescence quantum yield (Φ_{exp}) was calculated from Equation (1). Here, *F* denotes the integral of the corrected fluorescence spectrum, *A* is the absorbance at the excitation wavelength, and *n* is the refractive index of the medium. The reference system used was rhodamine 6G in methanol ($\Phi_{ref} = 0.78$, $\lambda_{exc} = 488$ nm).

$$\Phi_{exp} = \Phi_{ref} \frac{F\{1 - \exp(-A_{ref} \ln 10)\} n^2}{F_{ref}\{1 - \exp(-A \ln 10\} n_{ref}^2} \quad (1)$$

Differential scanning calorimetry (DSC) was performed on a Netzsch DSC 200 PC/1/M/H Phox instrument equipped with an intracooler, allowing measurements from −65 °C up to 450 °C. The samples were examined at a scanning rate of 10 K min^{-1} by applying two heating and one cooling cycles. The apparatus was calibrated with indium (156.6 °C). Phase behaviour was studied by polarised light optical microscopy (POM) on a Leica DMLB microscope equipped with a Linkam LTS350 hot-stage and a Linkam TMS94 central processor. The XRD patterns were obtained with a pinhole camera (Anton–Paar) operating with a point-focussed Ni-filtered Cu–K_α beam. The samples were held in Linde-

mann glass capillaries (0.9 mm diameter) and heated, when necessary, with a variable-temperature oven. The patterns were collected on flat photographic film perpendicular to the X-ray beam. Spacings were obtained by Bragg's law.

General procedure for the synthesis of [BODDS-C$_n$benzyl] complexes (n=8, 12, 16): The sulfonate salt (1 equiv) was dissolved in DMF (2 mg mL^{-1}) and the C$_n$benzyl (1 equiv per negative charge) was added. The mixture was stirred at 60 °C overnight. After cooling, water was added and the precipitate was washed with water and dried under vacuum. BODDS-C$_{12}$benzyl and -C$_{16}$benzyl were recrystallised from hot DMSO, BODDS-C$_8$benzyl was recrystallised from CH_2Cl_2/AcOEt by slow evaporation of dichloromethane and BODDS-P$_{12}$gall was recrystallised from hot cyclohexane.

BODDS-C$_8$benzyl: Isolated yield: 53 %. ^{1}H NMR (DMSO, 300 MHz): δ=9.15 (s, 2H), 7.80 (s, 2H), 7.68 (s, 2H), 6.78 (s, 4H), 5.23 (s, 4H), 3.93 (t, ^3J=6.3 Hz, 8H), 3.83–3.79 (m, 10H), 2.66 (s, 3H), 2.62 (s, 6H), 2.59 (s, 6H), 1.72–1.58 (m, 12H), 1.41–1.25 (m, 60H), 0.83 ppm (t, ^3J=6.3 Hz, 18H); IR (ATR): $\tilde{\nu}$=2924 (s), 2853 (s), 1610 (s), 1464 (m), 1440 (s), 1389 (m), 1306 (m), 1195 (s), 1147 (m), 1126 (m), 1119 (s), 1086 (s), 1018 (s), 997 (vs), 657 (s), 620 cm^{-1} (m); UV/Vis (CH_2Cl_2): λ (ε)=279 (7100), 314 (7000), 365 (8200), 507 nm (73400 M^{-1}cm^{-1}); elemental analysis calcd (%) for $C_{84}H_{137}BF_2N_6O_{12}S_2$: C 65.64, H 9.05, N 5.47; found: C 65.95, H 9.38, N 5.69.

BODDS-C$_{12}$benzyl: Isolated yield: 73 %. ^{1}H NMR (DMSO, 300 MHz): δ=9.14 (s, 2H), 7.79 (s, 2H), 7.67 (s, 2H), 6.77 (s, 4H), 5.23 (s, 4H), 3.93 (t, ^3J=6.0 Hz, 8H), 3.83–3.78 (m, 10H), 2.66 (s, 3H), 2.62 (s, 6H), 2.59 (s, 6H), 1.73–1.58 (m, 12H), 1.41–1.25 (m, 108H), 0.83 ppm (t, ^3J=6.1 Hz, 18H); IR (ATR): $\tilde{\nu}$=2945 (m), 2918 (s), 2850 (s), 1592 (m), 1536 (m), 1506 (m), 1466 (s), 1442 (m), 1227 (m), 1194 (s), 1116 (s), 1087 (s), 1019 (s), 996 (vs), 655 cm^{-1} (vs); UV/Vis (CH_2Cl_2): λ (ε)=278 (7400), 312 (6700), 363 (7600), 507 nm (85200 M^{-1}cm^{-1}); elemental analysis calcd (%) for $C_{108}H_{185}BF_2N_6O_{12}S_2$: C 69.23, H 10.01, N 4.49; found: C 69.59, H 10.35, N 4.78.

BODDS-C$_{16}$benzyl: Isolated yield: 72 %. ^{1}H NMR (DMSO, 400 MHz, 60 °C): δ=9.09 (s, 2H), 7.74 (s, 2H), 7.66 (s, 2H), 6.75 (s, 4H), 5.21 (s, 4H), 3.91 (t, ^3J=6.2 Hz, 8H), 3.83–3.78 (m, 10H), 2.66 (s, 3H), 2.62 (s, 3H), 2.59 (s, 3H), 1.73–1.58 (m, 12H), 1.41–1.25 (m, 156H), 0.83 ppm (t, ^3J=6.4 Hz, 18H); IR (ATR): $\tilde{\nu}$=2949 (m), 2915 (s), 2847 (s), 1599 (m), 1540 (m), 1510 (m), 1465 (s), 1442 (m), 1412 (w), 1221 (m), 1187 (s), 1123 (s), 1090 (s), 1020 (s), 1000 (vs), 655 cm^{-1} (vs); UV/Vis (CH_2Cl_2): λ (ε)= 276 (8600), 306 (7000), 364 (7000), 507 (68000 M^{-1}cm^{-1}); elemental analysis calcd (%) for $C_{132}H_{233}BF_2N_6O_{12}S_2$: C 71.73, H 10.67, N 3.80; found: C 72.15, H 11.19, N 4.29.

BODDS-P$_{12}$gall: Isolated yield: 81 %. ^{1}H NMR (DMSO, 300 MHz): δ= 9.21 (s, 2H), 7.85 (s, 2H), 7.71 (s, 2H), 7.13 (s, 4H), 6.29 (dd, ^3J=17.2, ^3J=1.9 Hz, 4H), 6.14 (dd, ^3J=17.4, ^3J=10.2 Hz, 4H), 5.91 (dd, ^3J=9.9, ^3J=1.4 Hz, 4H), 4.58 (s, 8H), 4.07 (t, ^3J=6.9 Hz, 8H), 3.97 (t, ^3J=6.0 Hz, 8H), 3.90 (t, ^3J=6.3 Hz, 4H), 3.84 (s, 6H), 2.66 (s, 3H), 2.61 (s, 6H), 2.59 (s, 6H), 1.74–1.54 (m, 24H), 1.45–1.22 (m, 88H), 0.83 ppm (t, ^3J=6.3 Hz, 6H); IR (ATR): $\tilde{\nu}$=2920 (vs), 2851 (vs), 1726 (vs), 1586 (m), 1536 (m), 1500 (m), 1467 (m), 1429 (m), 1408 (m), 1334 (m), 1309 (m), 1195 (vs), 1115 (s), 1087 (m), 1021 (m), 1000 (vs), 809 (m), 762 (m), 656 cm^{-1} (vs); UV/Vis (CH_2Cl_2): λ (ε)=275 (20300), 359 (10000), 507 nm (76000 M^{-1}cm^{-1}); elemental analysis calcd (%) for $C_{116}H_{185}BF_2N_6O_{20}S_2$: C 66.45, H 8.89, N 4.01; found: C 66.28, H 8.71, N 3.78.

The photopolymerisable sample was prepared by dissolving monomer BODDS-P$_{12}$gall and 1-hydroxycyclohexyl phenyl ketone (10 wt % of the monomer) as the photoinitiator in a solution of CH_2Cl_2. The solution was added dropwise onto a glass plate (evaporation of CH_2Cl_2) to form a thin red film. This resulting photopolymerisable sample was heated to an anisotropic state at 65 °C and then cooled to room temperature. Photopolymerisation of the columnar liquid crystals was carried out at 30 °C for 60 min under exposure to UV light (Lightning Cure LC8 HAMAMATSU, 365 nm, 5 mW cm^{-2}).

Acknowledgements

This work was jointly supported by the Université de Strasbourg through the European School of Polymer and Materials Chemistry (ECPM) and by the Centre National de la Recherche Scientifique (CNRS) of France. Financial support from MICINN-FEDER (Spanish project CTQ2009-09030) is gratefully acknowledged.

[1] a) K. Binnemans, *Chem. Rev.* **2005**, *105*, 4148–4204; b) T. Kato, N. Mizoshita, K. Kishimoto, *Angew. Chem.* **2006**, *118*, 44–74; *Angew. Chem. Int. Ed.* **2006**, *45*, 38–68; c) S. Laschat, A. Baro, N. Steinke, F. Giesselmann, C. Hägele, G. Scalia, R. Judele, E. Kapatsina, S. Sauer, A. Schreivogel, M. Tosconi, *Angew. Chem.* **2007**, *119*, 4916–4973; *Angew. Chem. Int. Ed.* **2007**, *46*, 4832–4887; d) J. W. Goodby, I. M. Saez, S. J. Cowling, V. Görtz, M. Draper, A. W. Hall, S. Sia, G. Cosquer, S.-E. Lee, E. P. Raynes, *Angew. Chem.* **2008**, *120*, 2794–2828; *Angew. Chem. Int. Ed.* **2008**, *47*, 2754–2787.

[2] L. Schmidt-Mende, A. Fechtenkötter, K. Müllen, E. Moons, R. H. Friend, J. D. MacKenzie, *Science* **2001**, *293*, 1119–1124.

[3] a) M. Yoshio, T. Mukai, H. Ohno, T. Kato, *J. Am. Chem. Soc.* **2004**, *126*, 994–995; b) T. Ichikawa, M. Yoshio, A. Hamasaki, T Mukai, H. Ohno, T. Kato, *J. Am. Chem. Soc.* **2007**, *129*, 10662–10663.

[4] Y. Abu-Lebdeh, A. Abouimrane, P.-J. Alarco, M. Armand, *J. Power Sources* **2006**, *154*, 255–261.

[5] a) N. Yamanaka, R. Kawano, W. Kubo, T. Kitamura, Y. Wada, M. Watanabe, S. Yanagida, *Chem. Commun.* **2005**, 740–742; b) R. Kawano, M. K. Nazeeruddin, A. Sato, M. Graetzel, M. Watanabe, *Electrochem. Commun.* **2007**, *9*, 1134–1138.

[6] a) W. Li, J. Zhang, B. Li, M. Zhang, L. Wu, *Chem. Commun.* **2009**, 5269–5271; b) N. Canilho, M. Scholl, H.-A. Klok, R. Mezzenga, *Macromolecules* **2007**, *40*, 8374–8383.

[7] F. Camerel, P. Strauch, M. Antonietti, C. F. J. Faul, *Chem. Eur. J.* **2003**, *4* 3764–3771.

[8] a) K. Goossens, P. Nockemann, K. Driesen, B. Goderis, C. Görller-Walrand, K. Van Hecke, L. Van Meervelt, E. Pouzet, K. Binnemans, T. Cardinaels, *Chem. Mater.* **2008**, *20*, 157–268; b) P. H. J. Kouwer, T. Swager, *J. Am. Chem. Soc.* **2007**, *129*, 14042–14052.

[9] a) F. Lo Celso, I. Pibiri, A. Triolo, R. Triolo, A. Pace, S. Biscemi, N. Vivona, *J. Mater. Chem.* **2007**, *17*, 1201–1208; b) D. Ster, U. Baumeister, J. Lorenzeo Chao, C. Tschierke, G. Israel, *J. Mater. Chem.* **2007**, *17*, 3393–3400.

[10] H. Ohno, *Bull. Chem. Soc. Jpn.* **2006**, *79*, 1665–1680.

[11] Y. Kamikawa; T. Kato, *Langmuir* **2007**, *23*, 274–278; T. Kato, *Langmuir* **2007**, *23*, 274–278.

[12] a) M. Yoshio, T. Mulai, K. Kanie, M. Yoshizawa, H. Ohno, T. Kato, *Adv. Mater.* **2002**, *14*, 351–354; b) T. Kato, *J. Am. Chem. Soc.* **2006**, *128*, 5570–5577.

[13] a) R. Ziessel, G. Ulrich, A. Harriman, *New J. Chem.* **2007**, *31*, 496; b) R. Ziessel, *C. R. Acad. Sci. Chim.* **2007**, *10*, 622; c) G. Ulrich, R. Ziessel, A. Harriman, *Angew. Chem.* **2008**, *120*, 1202–1219; *Angew. Chem. Int. Ed.* **2008**, *47*, 1184–1201; d) A. Loudet, K. Burgess, *Chem. Rev.* **2007**, *107*, 4891.

[14] a) G. Ulrich, C. Goze, M. Guardigli, A. Roda, R. Ziessel, *Angew. Chem.* **2005**, *117*, 3760–3764; *Angew. Chem. Int. Ed.* **2005**, *44*, 3694–3698; b) G. Ulrich, C. Goze, S. Goeb, P. Retailleau, R. Ziessel, *New J. Chem.* **2006**, *30*, 982; c) G. Ulrich, S. Goeb, A. De Nicola, P. Retailleau, R. Ziessel, *Synlett* **2007**, 1517.

[15] a) T. Rousseau, A. Cravino, J. Roncali, T. Bura, G. Ulrich, R. Ziessel, *Chem. Commun.* **2009**, 1673; b) T. Rousseau, A. Cravino, J. Roncali, T. Bura, G. Ulrich, R. Ziessel, *J. Mater. Chem.* **2009**, *19*, 2298; c) D. Kumaresan, R. P. Thummel, T. Bura, G. Ulrich, R. Ziessel, *Chem. Eur. J.* **2009**, *15*, 6335.

[16] *The Handbook: A Guide to Fluorescent Probes and Labeling Technologies*, 10th ed., R. P. Haughland, Invitrogen, **2005**, http ://www.probes.invitrogen.com.

[17] T. Gareis, C. Huber, O. S. Wolfbeis, J. Daub, *Chem. Commun.* **1997**, 1717—1718.

[18] A. Hepp, G. Ulrich, R. Schmechel, H. von Seggern, R. Ziessel, *Synth. Met.* **2004**, 146, 11–15; L. Bonardi, H. Kanaan, F. Camerel, P. Jolinat, P. Retailleau, R. Ziessel, *Adv. Funct. Mater.* **2008**, *18*, 401–413.
[19] a) F. Camerel, L. Bonardi, G. Ulrich, L. Charbonnière, B. Donnio, C. Bourgogne, D. Guillon, P. Retailleau, R. Ziessel, *Chem. Mater.* **2006**, *18*, 5009–5021; b) F. Camerel, L. Bonardi, M. Schmutz, R. Ziessel, *J. Am. Chem. Soc.* **2006**, *128*, 4548–4549.
[20] a) C. F. J. Faul, M. Antonietti, *Chem. Eur. J.* **2002**, *8*, 2764; b) C. F. J. Faul, M. Antonietti, *Adv. Mater.* **2003**, *15*, 673.
[21] F. Camerel, G. Ulrich, J. Barberá, R. Ziessel, *Chem. Eur. J.* **2007**, *13*, 2189–2200.
[22] F. Camerel, C. F. J. Faul, *Chem. Commun.* **2003**, 1958–1960.
[23] J.-H. Olivier, F. Camerel, J. Barberá, P. Retailleau, R. Ziessel, *Chem. Eur. J.* **2009**, *15*, 8163–8174.
[24] M. Yoshio, T. Kagata, K. Hoshino, T. Mukai, H. Ohno, T. Kato, *J. Am. Chem. Soc.* **2006**, *128*, 5570–5577.
[25] J. H. Boyer, A. M. Haag, G. Sathyamoorthi, M.-L. Soong, K. Thangaraj, T. G. Pavlopoulos, *Heteroat. Chem.* **1993**, *4*, 39–49.
[26] a) A. Harriman, L. J. Mallon, S. Goeb, G. Ulrich, R. Ziessel, *Chem. Eur. J.* **2009**, *15*, 4553–4564; b) A. Harriman, L. J. Mallon, R. Ziessel, *Chem. Eur. J.* **2008**, *14*, 11461–11473.
[27] F. Würthner, C. Bauer, V. Stepanenko, S. Yagai, *Adv. Mater.* **2008**, *20*, 1695–1698.
[28] J. Olmsted, *J. Phys. Chem.* **1979**, *83*, 2581–2584.
[29] S. Frein, F. Camerel, R. Ziessel, J. Barberá, R. Deschenaux, *Chem. Mater.* **2009**, *21*, 3950–3959.
[30] F. Camerel, J. Barberá, J. Otsuki, T. Tokimoto, Y. Shimazaki, L.-Y. Chen, S.-H. Liu, M.-S. Lin, C.-C. Wu, R. Ziessel, *Adv. Mater.* **2008**, *20*, 3462–3467.

Received: February 8, 2010
Published online: May 18, 2010

